JOURNAL OF SOLID STATE CHEMISTRY **122,** 87–94 (1996)
ARTICLE NO. 0086

Structural and Magnetic Phase Transitions of the 2D Ferromagnetic Fluoride Tl_2CuF_4

P. Núñez,*,[1] M. Morales-Escobar,* T. Roisnel,† J. M. Kiat,†,‡ R. Saez-Puche,§ H. Guengard,** J. Grannec,** and A. Tressaud**

*Departamento de Química Inorgánica, Universidad de La Laguna, 38208, La Laguna, Canary Islands, Spain; †Laboratoire Leon Brillouin, CEA-CNRS, CE-Saclay, 91191 Gif-Sur-Yvette Cedex, France; ‡Laboratoire de Chimie-Physique du Solide, Ecole Centrale de Paris, Grande Voie des Vignes, 92295 Chatenay-Malabry Cedex, France; §Departamento de Química Inorgánica, Facultad de Química, Universidad Complutense, 28040 Madrid, Spain; and **ICMCB, Université de Bordeaux I, Av. Dr. A. Schweitzer, 33608 Pessac Cedex, France

Received August 11, 1995; in revised form November 20, 1995; accepted November 28, 1995

A new transition phase has been observed in the copper complex fluoride, Tl_2CuF_4, with the K_2NiF_4-derived structure. A Rietveld refinement of the room-temperature X-ray powder pattern in the *I*4/*mmm* space group [a = 4.206(2) Å; c = 13.673(5) Å] has confirmed the antiferrodistortive arrangement of the e_g orbitals of Cu^{2+}. Around 200 K a structural phase transition to a low-temperature monoclinic phase has been evidenced by DSC and X-ray diffraction [space group *I*2/*m*, a = 4.182(2) Å, b = 4.183(2) Å, c = 13.492(6) Å; β = 94.564(4)°]. Tl_2CuF_4 exhibits ferromagnetic properties below T_c = 10 K. The dependence of the magnetization on the applied field is characterized at 1.7 K by a coercive field of 2.5 × 10^{-2} T and a remanent magnetization of 0.6 μ_B. The phase sequence has been compared with those found in La_2CuO_4-type compounds.

1. INTRODUCTION

The well-known K_2NiF_4 structure-type can be visualized as containing alternating perovskite ($KNiF_3$) and rock-salt (KF) blocks, which results in ninefold coordination for K^+ and octahedral coordination for Ni^{2+}. The relatively strong Ni–F–Ni superexchange interactions in the $NiF_{4/2}$ planes of the perovskite layers produces a 2D magnetically layered system (1). The structure may also be described as a perovskite disconnected in one direction. A_2CuF_4 (A = K, Rb, Cs, NH_4) compounds derive from this structural type, but the presence of Cu^{2+} ion induces an axial elongation of the [CuF_6] octahedra due to a strong Jahn–Teller effect (Fig. 1).

From the first structural determination of K_2CuF_4 (2) it was pointed out that the existence of a large unit cell was required for a complete indexing of the diffraction pattern (3). The [CuF_6] octahedra showed a tetragonal distortion with the elongated axis being alternately oriented along a and b axes (4). More recently, from neutron diffraction data a multidomain structure based on the displacements of F atoms (5) was proposed. These displacements reduce the symmetry from the tetragonal to the orthorhombic, which may be attributed to the two possible orientations of the Cu(II) e_g orbitals relative to the crystallographic a and b axes. However, an EPR investigation (6) does not support these results and, furthermore, in a structural redetermination by single-crystal X-ray diffraction (7), no superstructure reflections were detected, corresponding to the multidomain model.

In the present paper, we have studied the structure and magnetic properties of the compound Tl_2CuF_4, correlating the magnetic behavior to the structural features. We have also investigated a structural phase transition that takes place at low temperature and that has not been found in other isostructural A_2CuF_4 (A = K, Rb, Cs, NH_4) compounds.

2. EXPERIMENTAL

Sample Preparation

Tl_2CuF_4 powder was prepared by heating, at 300°C for 15 h, a stoichiometric mixture of TlF and CuF_2, in a platinum tube sealed under an argon atmosphere. A pure phase, checked by X-ray diffraction, was obtained after annealing under the same reaction conditions.

Diffraction Data

X-ray diffraction experiments were realized on a high-resolution, two-axis goniometer with Bragg–Brentano geometry and monochromated Cu$K\beta$ radiation issued from an 18 kW rotating anode. The Cu$K\beta$ radiation was used in order to avoid the interferences occurring between the Cu$K\alpha_1$ and $K\alpha_2$ doublet and a possible splitting of the

[1] To whom all correspondence should be addressed.

0022-4596/96 $18.00

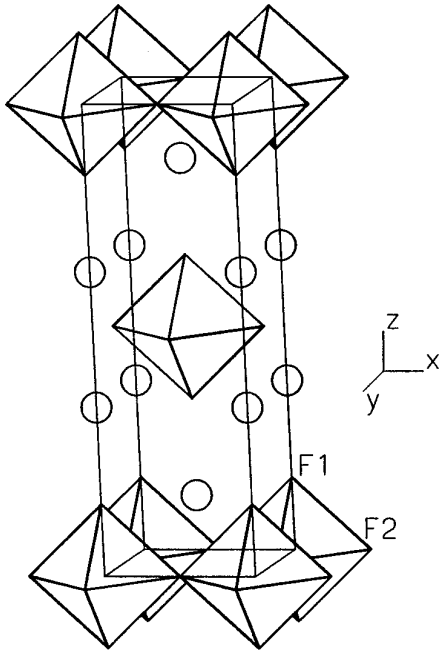

FIG. 1. Structure of K_2NiF_4.

Bragg peaks due to a lowering of symmetry of the studied compound. Diffraction patterns were collected in the 300–10 K temperature range using a helium cryostat.

Neutron diffraction experiments were performed at the Orphée reactor (Saclay, France), on the 3T2 high-resolution powder diffractometer for the structural phase transition study (λ = 1.2259 Å) and on the 2-axis G41 device for the magnetic part (λ = 2.426 Å) (8). Neutron data were analyzed with the Rietveld-type Fullprof program (9), and the following neutron scattering lengths: b_{Tl} = 0.8776×10^{-12} cm, b_{Cu} = 0.7718×10^{-12} cm, and b_F = 0.5650×10^{-12} cm. (10).

Thermal Analysis

Differential scanning calorimetry (DSC) has been performed with a Seiko 220C calorimeter using an aluminum container and corundum as a reference in the room temperature–120 K temperature range with a heating and cooling speed of 5 K min^{-1}.

Magnetic Measurements

Magnetic susceptibility measurements were taken with a SQUID Quantum Design magnetometer from 1.7 to 350 K; the equipment was calibrated with Pd and $Hg[Co(SCN)_4]$ as standards, and the data were corrected for ionic diamagnetism. The magnetization of this phase was determined as a function of the magnetic field from −4.5 to 4.5 T at different temperatures down to 1.7 K.

3. STRUCTURAL FEATURE OF THE Tl_2CuF_4 COMPOUND

Description of the Room-Temperature Structure

The synthesis of Tl_2CuF_4 has been reported previously and its cell parameters determined (11, 12), but no further studies have been reported in the literature.

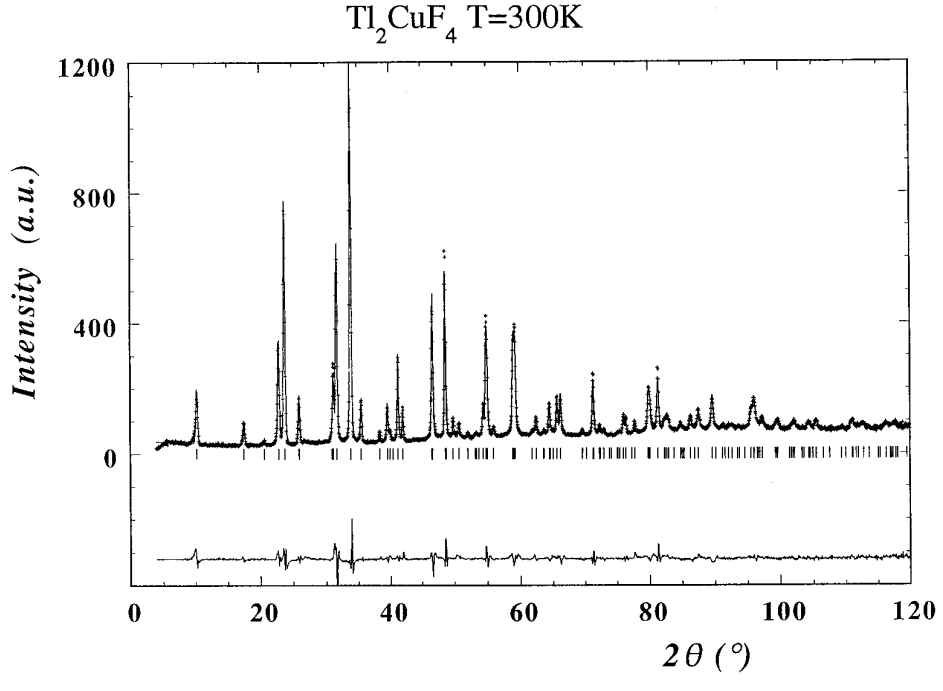

FIG. 2. Neutron powder diffraction patterns at room temperature (observed, calculated, and difference profile).

Tl_2CuF_4 crystallizes with the tetragonal symmetry in the $I4/mmm$ space group (No. 139). The refinement of the neutron powder diffraction data at room temperature (Fig. 2) has been carried out starting from the isostructural model of K_2CuF_4 (7). With respect to the potassium compound (K_2CuF_4: $a = 4.147(2)$ Å; $c = 12.73(3)$ Å), the unit cell parameters are increased due to the fact that the ionic radius of Tl^+ is slightly larger than that of the K^+ ion ($rTl^+ = 1.73$ Å; $rK^+ = 1.69$ Å, in nine coordination (13)), and also to the existence of an electronic lone pair on Tl^+. Tl_2CuF_4 consists of layers of octahedra sharing the four equatorial corners. Along the c direction the $CuF_{4/2}$ layers are shifted one layer relative to each other and separated by a Tl_2F_2 layer. Crystallographic data, atomic positions, and isotropic thermal Debye–Waller factors of Tl_2CuF_4 are listed in Table 1. Thallium and copper atoms as well as axial fluorine atoms (F1) are well located on special positions, 4*e*, 2*a*, and 4*e*, respectively. However, two models can be considered for the equatorial fluorine atoms, both in the same space group, depending on whether these atoms are located in 4*c* sites (model I) or in 8*i* sites (model II) (Fig. 3). In model I, the four Cu–F_{eq} distances (2.10 Å) are identical, with a D_{4h} symmetry and lead to a ferrodistortive arrangement (8) as shown in Fig. 3a. On the other hand, if F2 atoms are shifted off from the middle of the edge (from the $\frac{1}{2}$, 0, 0 position), the symmetry of the Cu(II) site is lowered to a D_{2h} symmetry (model II). In the latter case, due to the change of the site multiplicity, the F2 atoms, which are located in 8*i* sites, have a half-occupancy factor. As described in Fig. 3b, there are two different Cu–F distances in the *ab* plane (1.914 and 2.24 Å), which are in better agreement with a Jahn–Teller ion environment, and therefore the antiferrodistortive model II should be preferred with the long axial CuF2 bonds alternatively directed along *a* and *b* directions. It should be noticed that the isotropic thermal Debye–Waller factor of the F2 atom is reduced when the F atoms are shifted from the 4*c* site (3.89(55)) to the 8*i* site (2.04(68)), as shown in Table 1.

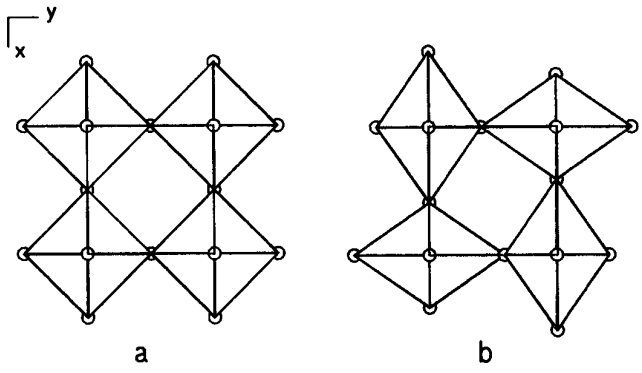

FIG. 3. Schematic representation of (a) ferrodistorsive and (b) antiferrodistorsive arrangement.

Phase Transition Study

Two successive phase transitions (14, 15) have been evidenced in $La_{2-x}Ba_xCuO_{4+\delta}$ phases, which are high-temperature superconductors, and they are also derived from the K_2NiF_4 structural type:

$$I4/mmm \text{ (HTT)} \leftrightarrow Bmab \text{ (LTO)} \leftrightarrow P4_2/ncm \text{ (LTT)}.$$

Due to the mismatch between the two types of layers forming the structure, the driving force of these phase transitions could be a minimization of the resulting strain energy (14). Moreover, these transitions are very much influenced by Ba doping. It is worth noting that these transitions have not been observed for A_2CuF_4 (A = K, Rb) fluorides, so far.

However, in the case of Tl_2CuF_4, X-ray powder diffraction patterns recorded between room temperature and

TABLE 1

Cell Parameters, Atomic Positions, Isotropic Thermal Parameters, and Selected Distances Obtained from Rietveld Refinement of Neutron Powder Diffraction Data at Room Temperature

Space group = $I\,4/mmm$ (No. 139) $a = 4.206(2)$ Å, $c = 13.673(5)$ Å

Atom	site (with occupancy)	x	y	z	B_{eq} (Å^2)
Tl	4*e*	0	0	0.3535(2)	1.77(5)
Cu	2*a*	0	0	0	0.91(18)
F1	4*e*	0	0	0.1399(2)	1.51(41)
F2 (model I)	4*c*	0.5	0	0	3.89(55)
(model II)	8*i*/2	0.4663(19)	0	0	2.04(68)

Cu–F1 = 1.914(3) Å Cu–F2 = 2.103(1) Å (Model I)
Cu–F2 = 1.961(8) and 2.244(8) Å (Model II)

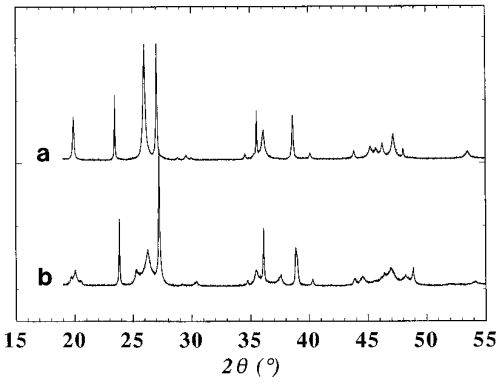

FIG. 4. X-ray powder diffraction patterns at (a) 300 K and (b) 10 K.

T = 10 K (Fig. 4) reveal the existence of a structural phase transition in this temperature range, and the low-temperature X-ray pattern can be indexed in a monoclinic unit cell related to the tetragonal one as follows:

$$a_m = 4.18 \text{ Å } (\approx a_t)$$
$$b_m = 4.18 \text{ Å } (\approx a_t)$$
$$c_m = 13.49 \text{ Å } (\approx c_t)$$
$$\beta = 94.41°.$$

In this unit cell, the observed reflections correspond to the $h + k + l = 2n$ selection rule, leading to a body-centered monoclinic cell. This monoclinic cell can be deduced from the tetragonal by a shearing stress of the (110) planes along the a direction. For the homologous cuprate series A_2CuO_4, only tetragonal/orthorhombic phase transitions have been described in the literature, but not a transition of the tetragonal ↔ monoclinic type.

The temperature-dependent splitting of the tetragonal (011) and (013) reflections is shown in Fig. 5. The experiments were carried out in the cooling mode from room temperature to 10 K.

The DSC measurement (Fig. 6), which is reproducibly obtained on cooling, revealed a diffuse signal between ca. 225 and 190 K with a maximum at $T_{tr} \approx 200$ K. In the heating run, a broader signal is observed in the same temperature range. This temperature T_{tr} can be related to the temperature from which a broadening of the (011) and (013) tetragonal Bragg reflections is observed when lowering the temperature (Fig. 5c).

In order to determine the low-temperature structure of Tl_2CuF_4, neutron diffraction experiments have been carried out at 16 K (Fig. 7). As was deduced from the room-temperature structure determination, one may assume that the low-temperature structure of Tl_2CuF_4 still consists of a stacking of antiferrodistortive octahedral layers. If we maintain the origin of the body-centered unit cell, the low-temperature structure of Tl_2CuF_4 can be described in the I 1 2/m 1 monoclinic space group, which is a nonconventional setting of the standard $C2/m$ space group (No. 12).

In Table 2 are listed the atomic positions, the isotropic temperature factors, and some selected Cu–F distances obtained from the Rietveld refinement of the low-temperature neutron data. The metallic atoms and Fl fluorine are located in special positions, whereas the shared fluorine atoms F2 and F3 are located in 4i and 4g sites, respectively, but both with a half-occupancy factor (model I). In the 4g crystallographic site, the F3 atoms exhibit a rather high isotropic temperature factor ($\beta = 0.99$ Å^2). However, when the F3 atoms are located in the 8j site, with a fourth occupancy factor (model II), the isotropic temperature factor

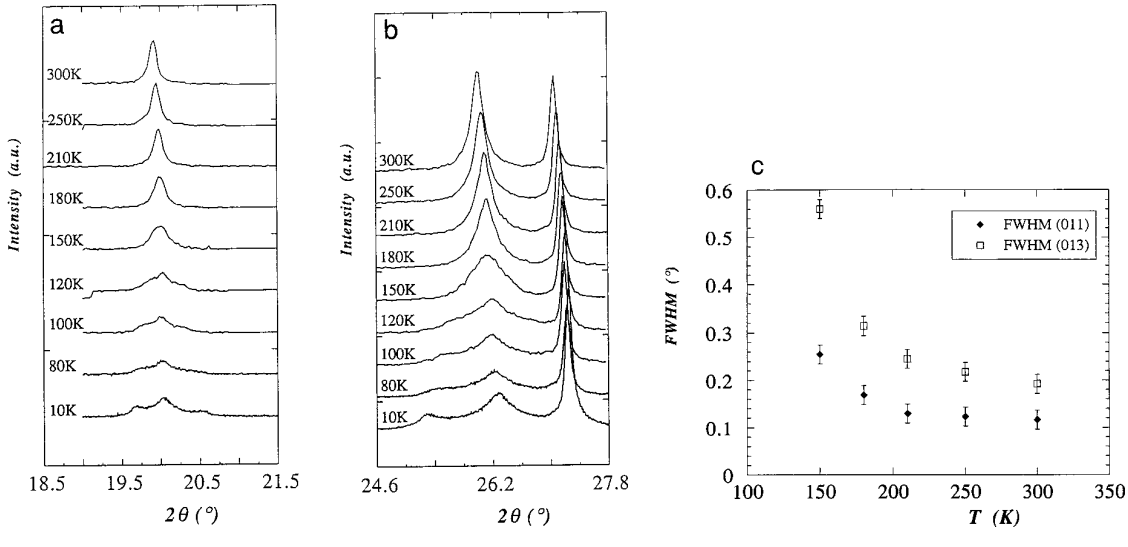

FIG. 5. Thermal variation of the tetragonal (a) (011) and (b) (013) reflection splitting and (c) FWHM.

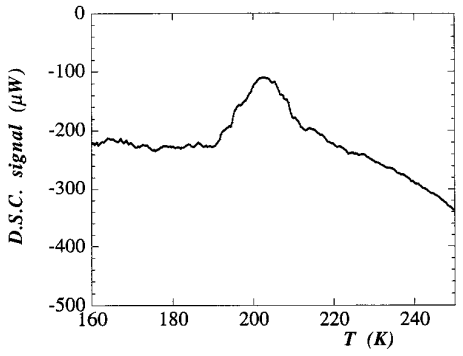

FIG. 6. Differential scanning calorimetry curve.

is reduced ($\beta = 0.68$ Å^2). In both models, the Cu–F3 distance is very short.

4. MAGNETIC PROPERTIES

The thermal variation of the reciprocal molar magnetic susceptibility, which is shown in Fig. 8, obeys a Curie–Weiss law above $T = 20$ K, providing the empirical parameters $C_m = 0.368$ and $\theta_p = 20$ K. This experimental value of the Curie constant, C_m, is consistent with the one calculated with the theoretical spin-only values (0.375).

The temperature dependence of the product of magnetic susceptibility and the temperature (χT) is shown in the inset of Fig. 8. The drastic increase of the χT product below 20 K and the positive value of the Curie constant are both indicative of the existence of ferromagnetic behavior.

Rushbrooke and Wood (16) have developed a high-temperature series expansion (HTSE), leading to the general equation

$$\frac{1}{X} = \frac{3\theta}{S(S+1)} \sum_{\theta} \frac{b_n}{n},$$

where X is the reduced magnetic susceptibility, given by $X = J\chi/Ng^2b^2$, θ is the reduced temperature, given by $\theta = kT/J$, g is the spectroscopic splitting factor, and b_n are the series expansion coefficients, which are given in a complex matricial form up to $n = 6$ for eight lattice types and different spin values ($S = \frac{1}{2}$–$\frac{5}{2}$), including both ferromagnetic and antiferromagnetic cases.

For ferromagnetic behavior with a square planar geometry and $S = \frac{1}{2}$, the general equation is given by

$$C/(\chi T) = 1.0 - 2.0\,\theta + 2.0\,\theta^2 - 1.3333\,\theta^3 + 0.25\,\theta^4 + 0.483\,\theta^5 + 0.0013\,\theta^6.$$

The best fitting of the thermal variation of the susceptibility to this equation allows us to determine the magnetic parameters: the magnetic exchange constant $J/k = +11.3$ K and the spectroscopic splitting factor $g = 2.04$.

We have carried out a study of the magnetization vs the magnetic field of the phase Tl_2CuF_4 at different tempera-

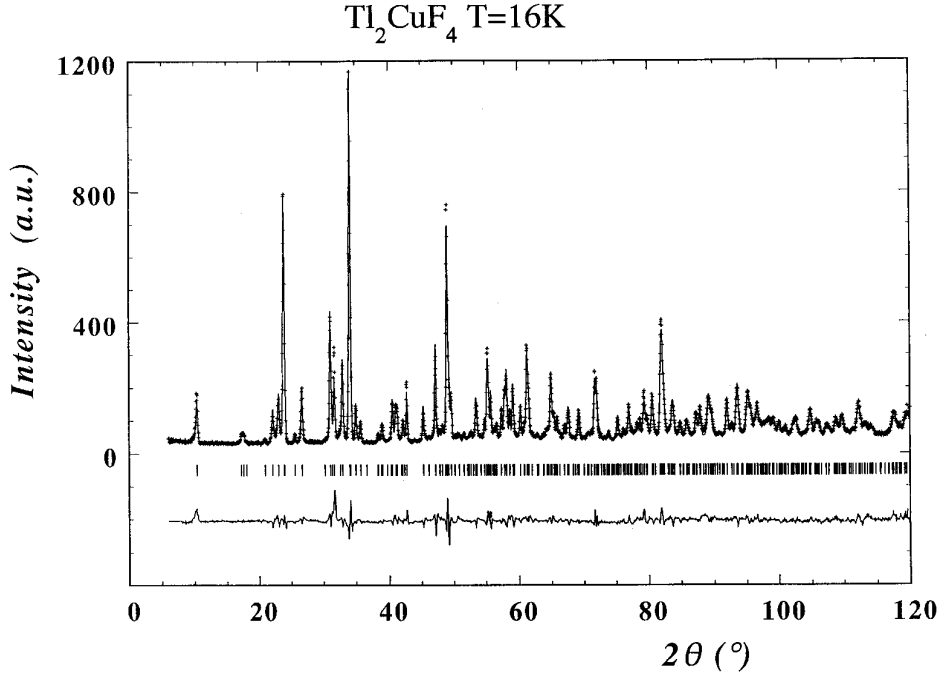

FIG. 7. Neutron powder diffraction patterns at $T = 16$ K (observed, calculated, and difference profile).

TABLE 2
Cell Parameters, Atomic Positions, Isotropic Thermal Parameters, and Selected Distances Obtained from Rietveld Refinement of Neutron Powder Diffraction Data at 16 K

Space group = $I2/m$(No. 12) a = 4.182(2) Å, b = 4.183(2) Å, c = 13.492(6) Å, β = 94.564(4)°

Atom	site (with occupancy)	x	y	z	B_{eq} (Å^2)
Cu	2a	0	0	0	0.33(5)
Tl	4i	−0.0126(1)	0	0.3530(2)	0.21(4)
F1	4i	0.0493(7)	0	0.1433(3)	0.53(6)
F2	4i/2	0.5367(21)	0	0.0004(10)	0.54(12)
F3	4g/2	0	0.5340(24)	0	0.99(14)
	8j/4	0.0188(63)	0.5365(26)	0.0015(21)	0.68(24)

Cu–F1 = 1.928(4) Å
Cu–F2 = 1.938(9) and 2.244(9) Å
Cu–F3 = 1.949(10) and 2.234(10) for F3 in 4g site (model I)
Cu–F3 = 1.941(11) and 2.245(11) for F3 in 8j site (model II)

tures. At 1.7 K the saturated magnetization is completely reached under a rather weak magnetic field (≈0.5 T). The value of saturated magnetization at 1.7 K is 0.90(5) μ_B, which implies that the unpaired spins of Cu(2+) ions are parallel. From the dependence of the magnetization with temperature, the curves $M^2 = f(H/M)$ allow us to determine the Curie temperature as 10 ± 1 K.

In order to detect possible magnetic hysteresis phenom-

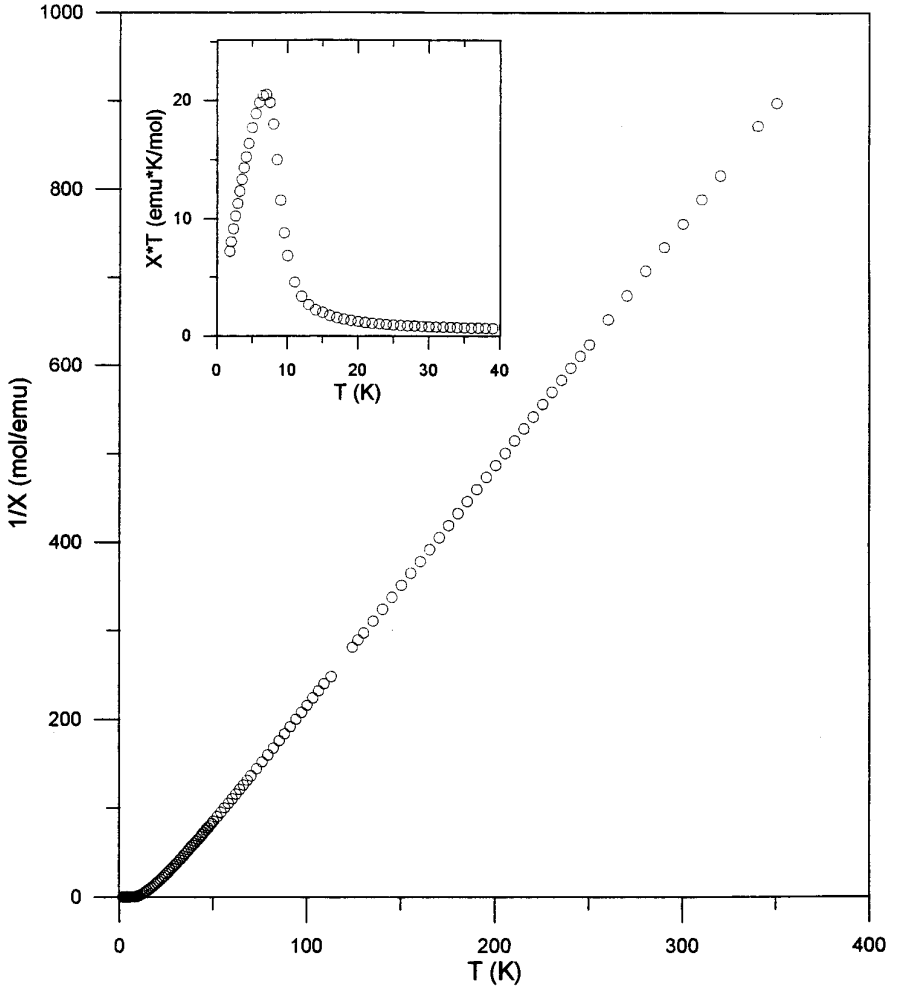

FIG. 8. Reciprocal magnetic susceptibility vs temperature in the 2–300 K range (the inset represents the thermal variation of the χT product).

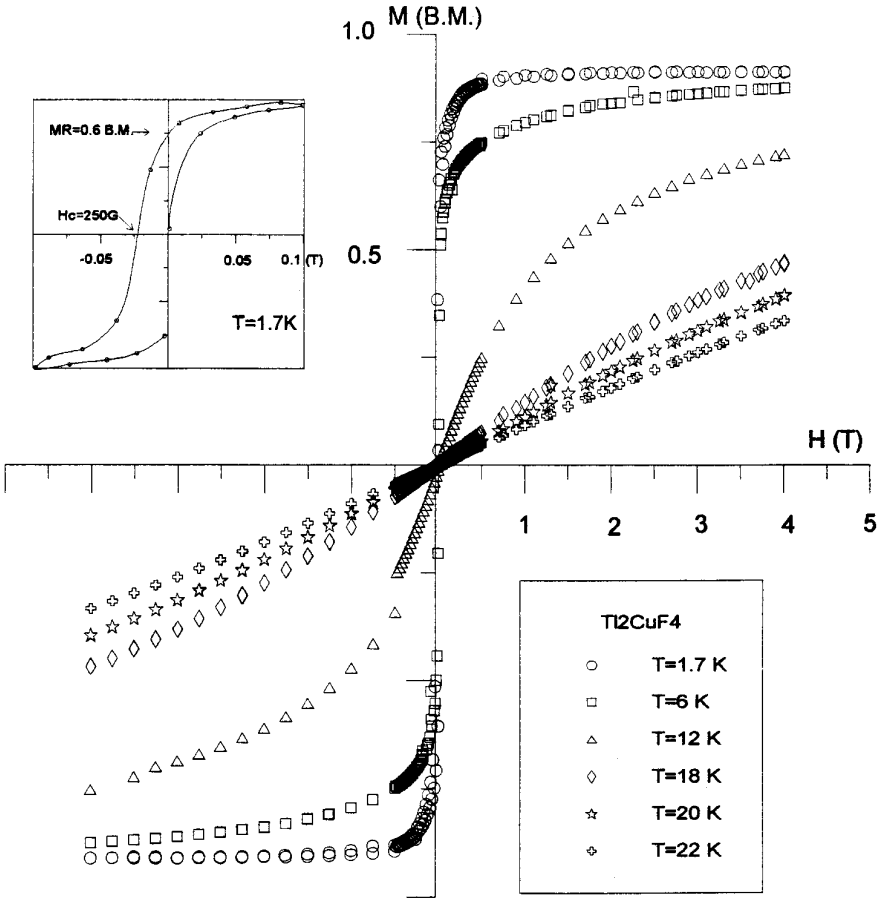

FIG. 9. Magnetization vs magnetic field ranging from −4.5 to +4.5 T at different temperatures (the inset represents isotermal hysteresis $M = f(H)$ at 2 K, in order to show the coercive field ($H_C = 2.5 \times 10^{-2}$ T) and the remanent magnetization ($M_R = 0.6\ \mu_B$)).

ena, we have measured the change of magnetization under both positive and negative magnetic fields (Fig. 9). It may be noticed from the inset of Fig. 9 that a weak hysteresis phenomenon has been observed in the isothermal $M = f(H)$ curve at 1.7 K, which is characterized by a coercive field H_c of 2.5×10^{-2} T and a remanent magnetization M_R of 0.6 μ_B. These values are indicative of a soft ferromagnetic material.

A neutron powder diffraction study has been performed in the 1.5–11 K temperature range in order to determine the magnetic structure of this Tl_2CuF_4 ferromagnetic compound. Weak magnetic contributions are observed in the ordered magnetic state on some nuclear Bragg peaks. However, due to preferential orientation effects in this layered compound and to the low magnetic moments on the Cu(2+), the magnetic moment direction and modulus cannot be obtained from the low-temperature neutron pattern.

For K_2CuF_4 in which an antiferrodistortive octahedral arrangement was also observed, a similar atomic orbital ordering has been proposed (17), which is supported by the crystallographic results and confirmed by NMR studies in the case of Rb_2CuF_4 (18). The Goodenough–Kanamori–Anderson rules (19) on superexchange interactions allow us to explain the ferromagnetic behavior of Tl_2CuF_4 phases in terms of a peculiar atomic orbital arrangement for the cupric ion. Cu(2+) has an electronic configuration (d^9), leading to a strong Jahn–Teller effect. For an antiferrodistortive arrangement, it is possible to assume that d_z2 is the filled electronic orbital and that along the a and b axes the atomic d_z2 and $d_{x^2-y^2}$ orbital are alternated. The magnetic interaction mechanism involves the following ordering: $d_z2 - p\sigma - d_{x^2-y^2}$, which leads to a ferromagnetic behavior by delocalization superexchange (19). It can be noted that a ferrodistortive octahedral arrangement should have led to an antiferromagnetic behavior, which is an example of the close relationships between structure and physical properties.

Summarizing, it has been shown that Tl_2CuF_4 is a ferromagnetic fluoride deriving from the K_2NiF_4 structure by an antiferrodistortive arrangement of the e_g orbitals. For the first time a structural phase transition to a low-tem-

perature monoclinic phase has been evidenced in these systems.

REFERENCES

1. R. J. Birgeneau, J. Shalo, and G. Shirane, *J. Appl. Phys.* **41,** 1303 (1970).
2. K. Knox, *J. Chem. Phys.* **30,** 991 (1959).
3. R. Haegele and D. Babel, *Z. Anorg. Allg. Chem.* **409,** 11 (1974).
4. C. Friedel and D. Reinen, *Z. Anorg. Allg. Chem.* **407,** 193 (1974).
5. M. Hidaka and P. J. Walter, *Solid State Commun.* **31,** 383 (1979).
6. D. Reinen and M. Weitzel, *Inorg. Chem.* **20,** 2750 (1981).
7. E. Herdtweck and D. Babel, *Z. Anorg. Allg. Chem.* **474,** 113 (1981).
8. T. Roisnel, J. Rodríguez-Carvajal, M. Pinot, G. André, and F. Bourée, *Mater. Sci. Forum* **166,** 245 (1994).
9. J. Rodríguez-Carvajal, "Powder Diffraction Satellite Meeting of XV Congress of IUCr, Toulousse, France." Abs., p. 127. 1990.
10. V. F. Sears, *Neutron News* **3(3),** 26 (1992).
11. W. Rüdorff and D. Babel, *Naturwiss* **49,** 230 (1962).
12. W. Rüdorff, G. Lincke, and D. Babel, *Z. Anorg. Allg. Chem.* **320,** 150 (1963).
13. R. D. Shannon and C. T. Prewitt. *Acta Crystallogr. B* **25,** 925 (1969); R. D. Shannon, *Acta Crystallogr. A* **32,** 751 (1976).
14. J. D. Axe, A. H. Moudden, D. Hohlwein, D. E. Cox, K. Mohanty, A. R. Moodenbaugh, and Youwen Xu, *Phys. Rev. Lett.* **62(23),** 2751 (1989).
15. M. Douzi, *J. Phys. I* **1,** 743 (1991); J. F. Bringley; S. S. Trail, and B. A. Scott, *J. Solid State Chem.* **86,** 310 (1990).
16. G. S. Rushbrooke and P. J. Wood, *Mol. Phys.* **1,** 257 (1958).
17. D. J. Khomskii and K. J. Kugel, *Solid State Commun.* **13,** 763 (1973).
18. L. C. Gupta, R. Vijayaraghavan, S. D. Damle, V. R. K. Rao, Le Dang, Khoi, and P. Veillet, *J. Magn. Reson.* **17,** 41 (1975).
19. P. W. Anderson, *Phys. Rev.* **115,** 2(1959); J. Kanamori, *Phys. Chem. Solids* **10,** 87 (1959); J. B. Goodenough, "Magnetism and the Chemical Bond," Interscience, New York, 1963.